catalysts

MDPI

Article

Faster Microwave-Assisted Synthesis of Microspherical Carbons from Commercial and Biomass-Derived Carbohydrates

Aroldo J. Romero-Anaya [1], M. Dolores González [2], Judith Granados-Reyes [2], Leví E. Arrieche-Hernández [2] and Yolanda Cesteros [2,*]

[1] Eurecat, Centre Tecnològic de Catalunya, C/Marcel·lí Domingo, 43007 Tarragona, Spain; ajromero_1@yahoo.es
[2] Departament de Química Física i Inorgànica, C/Marcel·lí Domingo 1, Universitat Rovira i Virgili, 43007 Tarragona, Spain; mdolores.gonzalez@urv.cat (M.D.G.); judithcecilia.granados@urv.cat (J.G.-R.); leviemanuel.arrieche@urv.cat (L.E.A.-H.)
* Correspondence: yolanda.cesteros@urv.cat; Tel.: +34-977-559571

Abstract

Carbon microspheres were prepared by microwave-assisted hydrothermal treatment, at 180 °C, of commercial carbohydrates (saccharose, glucose, and xylose) and xylose extract obtained from almond shells with varying synthesis parameters. When 1.6 M aqueous solutions of commercial carbohydrates were used, 2–10 μm carbon microspheres were obtained from saccharose after 15 min, while a longer amount of time (60 min) and the addition of acid medium (1% *v*/*v* H_2SO_4, 1% *v*/*v* H_3PO_4) were needed to obtain carbon microspheres from commercial xylose and glucose ($\leq$ 1 μm). The higher reactivity of saccharose could be related to the formation, during heating, of fructose, which is more reactive than glucose and xylose. An increase in the acid concentration and in the carbohydrate concentration increased the formation and size of the microspheres. Comparative experiments with conventional heating did not produce a solid. Interestingly, when xylose extract obtained from almond shells was used, small carbon microspheres (1–3 μm) were obtained at a much lower concentration (0.2 M) and time (15 min) than with commercial xylose. This could be related to the acid medium used during extraction of xylose from the biomass. Activation of microspheres with CO_2 resulted in high-surface area materials (243–326 m^2/g) with great potential as catalytic supports.

Keywords: spherical carbons; microwaves; biomass valorization; xylose; glucose; saccharose

Academic Editor: Anjie Wang

Received: 10 August 2025
Revised: 9 September 2025
Accepted: 10 September 2025
Published: 15 September 2025

Citation: Romero-Anaya, A.J.; González, M.D.; Granados-Reyes, J.; Arrieche-Hernández, L.E.; Cesteros, Y. Faster Microwave-Assisted Synthesis of Microspherical Carbons from Commercial and Biomass-Derived Carbohydrates. *Catalysts* **2025**, *15*, 885. https://doi.org/10.3390/catal15090885

1. Introduction

Lignocellulosic biomass is one of the most important renewable resources, since it does not compete with food crops due to its non-edible nature and is less expensive than conventional agricultural feedstocks. For this reason, adequate upgrading strategies using new technologies are under research for the conversion of this type of biomass into high-value products.

The preparation of carbon materials with different morphologies from lignocellulosic biomass could be an excellent option for its valorisation. Specifically, the preparation of spherical carbons has become popular in recent years with respect to traditional carbon materials because they have interesting properties such as wear resistance, mechanical strength, good adsorption performance, purity, low ash content, a smooth surface, good fluidity, good packaging, a low pressure drop and a high bulk density [1–15]. Additionally,

their microporosity can be increased with tuneable pore size distribution using controlled procedures [1–4]. These properties have allowed spherical carbons to be used in many applications such as gas-phase adsorption [6], liquid-phase adsorption [7], energy storage [8], CO_2 storage [9], catalysis [10], photocatalysis [11], medicine [12], heavy metal wastewater treatment [13,14], and controlled drug delivery [15].

The preparation of spherical carbons has brought with it the use of different sources as precursors, like polymers [16], resorcinol–formaldehyde resin [17], polystyrene-based macroreticular ion-exchange resin spheres [18], or urea/formaldehyde resin [19], lignocellulosic biomass as natural biofibres [20], sugarcane [21], lettuce [22], waste peanut hull [23], or algae [24]. Taking into account that lignocellulosic wastes have gained importance in recent times, carbohydrates, such as lignin [25], cellulose [26], saccharose [3], glucose [27,28], fructose [29], and xylose [30], have also been used as raw materials for the synthesis of spherical carbon materials.

The most common methodology used to prepare spherical carbons is conventional hydrothermal treatment [31–34]. After the first publications at the beginning of the 20th century, which were specially focused on the coal formation mechanism [35,36], the first study about the formation of carbon microspheres with sizes of around 1.5 μm by the hydrothermal treatment of saccharose was published in 2001 [37]. Later, the preparation of carbon spheres from glucose or saccharose, loaded with noble-metal nanoparticles with sizes lower than 0.2 μm, was also reported [38].

In the last 20 years, the interest in the synthesis of spherical carbons by hydrothermal treatment has considerably increased. Sevilla et al. prepared spherical carbons using biomass [39], commercial cellulose [26], and commercial saccharose [40,41]. Titirici et al. prepared spherical carbons from different lignocellulosic materials such as sunflower stem, walnut shells, or olive stones [42,43], different commercial carbohydrates such as monosaccharides as xylose [30] and glucose [44,45], disaccharides such as saccharose [46] and maltose [30] and polysaccharides such as cellulose [43], amylopectin from potato starch [30], and aldehydes such as furfural and 5-HMF derived from thermal decomposition of carbohydrates [30,47]. In all these works, variables such as the hydrothermal treatment time, temperature or the concentration of the precursor have been studied [26,30,39–47]. The optimal time for the hydrothermal treatment by conventional heating was found to be around 24 h [3]. Microwave irradiation is becoming a reference technology in reducing preparation temperatures or times, significantly lowering costs in productive processes [48]. When applied to the preparation of solids, microwaves not only decrease the synthesis temperature or time, with the corresponding energy-saving, but can also modify the final properties of the solids [49–51]. For this reason, microwave technology has gained interest in recent decades as a powerful tool for the pyrolysis of different wastes or biomass [52–54]. Taking into account that carbon materials and their precursors are good microwave absorbers [55], many researchers have carried out investigations using microwave-assisted processes for the production, modification, and regeneration of carbon materials [39–47]. However, there are no references about the application of microwaves for the synthesis of carbon microspheres from carbohydrates or natural xylose extracted from lignocellulosic biomass.

In this work, microspherical carbons were prepared from commercial carbohydrates (xylose, glucose, and saccharose) and from xylose extract obtained from lignocellulosic biomass (almond shells) with microwave irradiation. The effect of the microwave irradiation time, the addition of different mineral acids to the aqueous solution medium (H_2SO_4, H_3PO_4), and the concentration of the carbohydrate on the preparation of the spherical carbons were analyzed. The activation of carbon microspheres with CO_2 was also studied.

2. Results and Discussion

Figure 1 shows the results obtained by heating 1.6 M aqueous solutions of commercial glucose, xylose, and saccharose to 180 °C with microwave irradiation and magnetic stirring for 15 and 60 min. Spherical carbons were obtained from saccharose after 15 min (S15) although the spheres were not well defined, showed variable sizes (2–10 μm), and presented poor formation. An increase in the microwave irradiation time to 60 min (S60) resulted in a higher formation, higher definition and more homogeneous sizes of spheres (4–7 μm) accompanied by the presence of some bigger spheres of around 12 μm. Therefore, we obtained spherical carbons from saccharose using microwaves at much shorter times than those used with conventional heating, for which longer times at the same temperature were required (12 or 24 h) [3]. On the other hand, carbon spheres were not formed when using commercial glucose or xylose in the same conditions independently of the heating time (G15, G60, X15, X60).

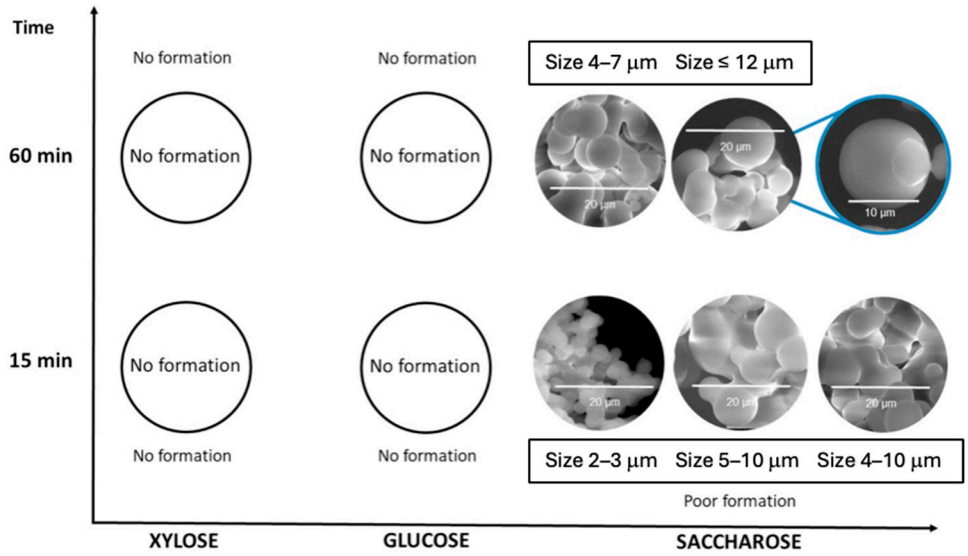

Figure 1. ESEM images of the carbon microspheres obtained by microwave-assisted hydrothermal treatment of 1.6 M aqueous solutions of commercial xylose, glucose, and saccharose at 180 °C under magnetic stirring for 15 and 60 min.

The mechanism of formation of carbon microspheres involves multiple steps (Figure 2). For disaccharides such as saccharose, an additional step is required. First, saccharose is hydrolysed into monocarbohydrates, glucose, and fructose [40]. Then, monocarbohydrates are dehydrated into furanic compounds, mainly 5-HMF (from glucose and fructose) and furfural (from xylose). Dehydrated compounds (5-HMF and furfural) react through several polymerization–condensation reactions until the formation of polyfuranic compounds is achieved. At the same time, depending on the hydrothermal conditions, aromatization reactions can occur and the carbon microspheres may form a polyaromatic network [56]. Under mild hydrothermal conditions, the main fragments consist of furanic and aliphatic groups [57], whereas at stronger hydrothermal conditions, the formation of phenolic domains is favoured [26]. The formation of a polyaromatic network is predominant in high-temperature reaction conditions [58]. The different behaviour observed for saccharose in aqueous solution with respect to xylose and glucose (Figure 1) should be related to the formation of fructose, which is more reactive for obtaining 5-HMF, and consequently, increases the yield for the formation of carbon microspheres [57].

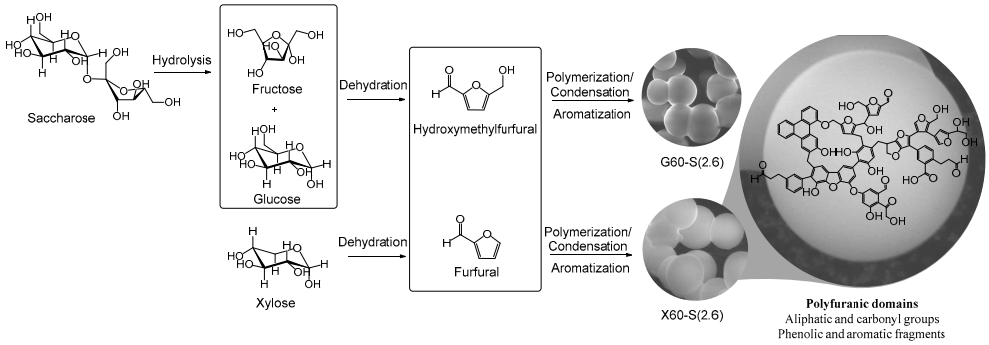

Figure 2. Proposed mechanism for the formation of carbon microspheres.

In order to obtain carbon microspheres from glucose and xylose under microwaves, we changed two preparation parameters: the addition of acid medium (1% v/v H_2SO_4, 1% v/v H_3PO_4, 25% v/v H_3PO_4) to the aqueous solution and the concentration of carbohydrate (2.6 M). Figures 3 and 4 show the results obtained for the samples of glucose and xylose, respectively, with microwaves at 180 °C for 60 min.

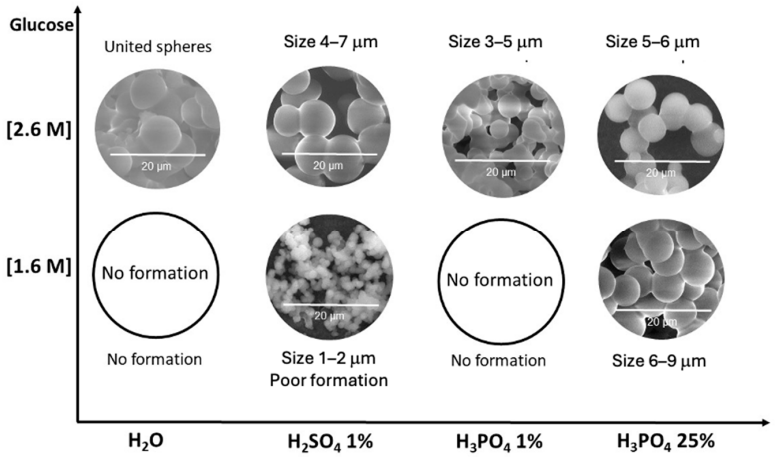

Figure 3. ESEM images of the carbon microspheres obtained by microwave-assisted hydrothermal treatment of 1.6 and 2.6 M aqueous solutions of commercial glucose with 1% v/v H_2SO_4, 1% v/v H_3PO_4, and 25% v/v H_3PO_4 at 180 °C under magnetic stirring for 60 min.

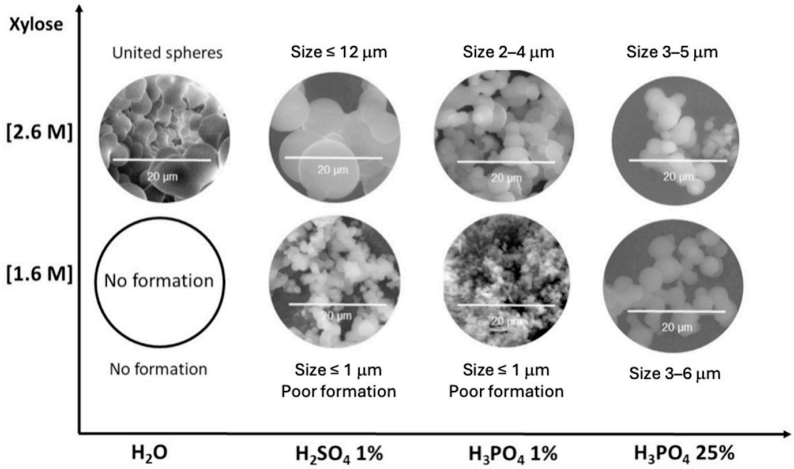

Figure 4. ESEM images of the carbon microspheres obtained by microwave-assisted hydrothermal treatment of 1.6 and 2.6 M aqueous solutions of commercial xylose with 1% v/v H_2SO_4, 1% v/v H_3PO_4 and 25% v/v H_3PO_4 at 180 °C under magnetic stirring for 60 min.

The addition of 1% v/v H_2SO_4 to the 1.6 M solution favoured the synthesis of small carbon spheres ($\leq$3 μm) from glucose (G60-S) and $\leq$1 μm from xylose (X60-S) but with poor formation. In contrast, by adding 1% v/v H_3PO_4 to the 1.6 M solution, small carbon spheres ($\leq$1 μm) at very low formation were obtained from xylose (X60-P, Figure 4) but not from glucose (G60-P, Figure 3). This can be related to the differences in the reactivities of the starting carbohydrates, since the number of decomposed species generated from the different saccharides during the hydrothermal treatment differed [40]. By increasing the concentration of H_3PO_4 to 25%, well-defined carbon spheres were obtained from both glucose (G60-P25) and xylose (X60-P25) with larger sizes (3–9 μm). Therefore, the acid medium increased the reaction rate during the hydrothermal treatment. This can be explained by the presence of hydronium ions from the acid, which catalyze the dehydration and further polymerization of 5-HMF [59]. Another study also reported an increase in the glucose decomposition at pH values between 1.5 and 2.2 at temperatures close to 200 °C [60].

The use of a higher concentration of the carbohydrate aqueous solution (2.6 M) facilitated the formation of undefined carbon spheres for both glucose (G60(2.6)) and xylose (X60(2.6)) but with a slightly higher definition, higher formation, and bigger size again for those obtained from glucose (Figures 2 and 3). Logically, when sugar concentration rose, polymerization also increased, as all the equilibriums were displaced towards the formation of the polymer. The addition of 1% v/v H_2SO_4 at a higher glucose concentration (2.6 M) increased the formation, the size (4–7 μm), and the definition of the carbon microspheres, while the addition of 1% v/v H_3PO_4 allowed their appearance with a size of 3–5 μm (Figure 2). By using the xylose precursor (2.6 M), an increase in the size, definition, and formation of the carbon microspheres was observed in both acid conditions (Figure 3). The increase in the concentration of H_3PO_4 to 25% increased the formation of spheres but with similar sizes with respect to those prepared with 1% v/v H_3PO_4. H_2SO_4 is a stronger and more dehydrating acid than H_3PO_4, so polymerization should be faster, and also dehydration should start faster, leading to bigger spheres.

Two acid-modified xylose samples (X120-S(2.6) and X120-P25(2.6)) were prepared at a longer microwave irradiation time (120 min) in order to study its effect on the formation of carbon microspheres at a higher concentration (2.6 M). The formation of spheres increased slightly but their size was similar (Figure 5).

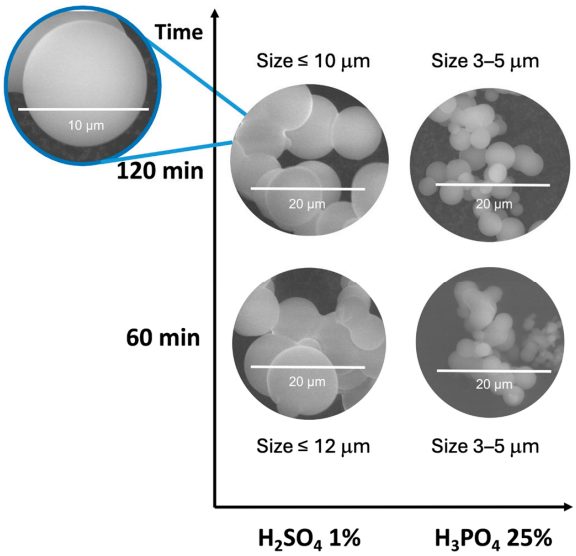

Figure 5. ESEM images of the carbon microspheres obtained by microwave-assisted hydrothermal treatment of 2.6 M aqueous solutions of commercial xylose with 1% v/v H_2SO_4 and 25% v/v H_3PO_4 at 180 °C under magnetic stirring for 60 and 120 min.

In order to more clearly observe the effect of microwaves on the formation of carbon microspheres, three samples were prepared by conventionally heating 2.6 M aqueous solutions of commercial xylose to 180 °C for 60 min (samples X60(2.6)C, X60-S(2.6)C, X60-P(2.6)C). The results are shown in Figure 6, compared to the corresponding samples prepared at the same conditions but with microwaves. Carbon spheres were not observed in any of the samples prepared by conventional heating. Therefore, the use of microwaves favoured the formation of the carbon microspheres. This could be explained by the higher homogeneity of the heating with microwaves, which allowed faster microspheres formation, reducing the preparation time, with the subsequent energy-saving, as observed in the preparation of other materials [46–48].

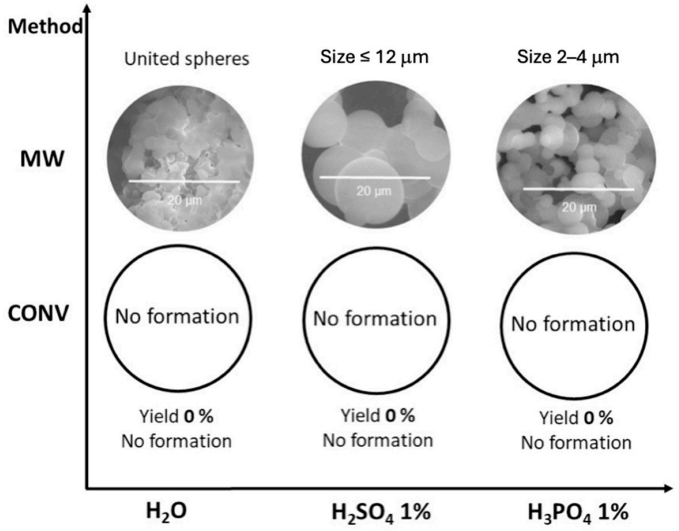

Figure 6. ESEM images of the carbon microspheres obtained by conventional (CONV) and microwave-assisted (MW) hydrothermal treatment of 2.6 M aqueous solutions of commercial xylose with 1% *v*/*v* H_2SO_4 and 1% *v*/*v* H_3PO_4 at 180 °C for 60 min.

Finally, natural xylose extract solution (36 g/L, approximately 0.2 M), obtained from almonds shells, was used for the preparation of spherical carbons with microwaves for 15 and 60 min (Figure 7).

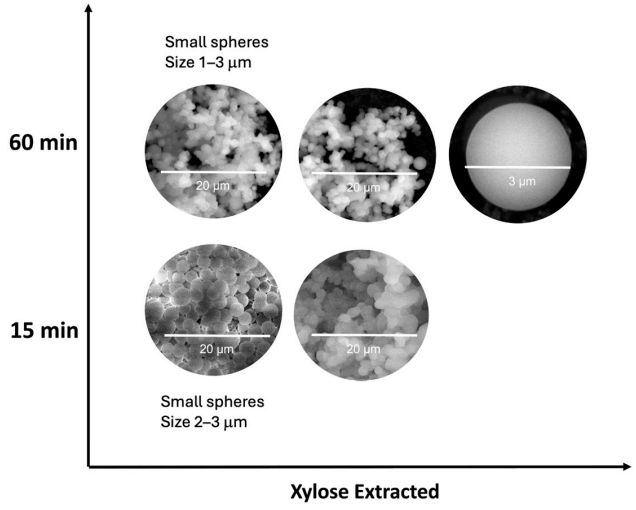

Figure 7. ESEM images of the carbon microspheres obtained by microwave-assisted hydrothermal treatment of natural xylose extract solutions at 180 °C for 15 and 60 min.

Interestingly, the results showed the formation of very small, well-defined carbon microspheres for both reaction times (≤1–3 μm). This contrasts with the results obtained with commercial xylose in which a much higher concentration was needed in aqueous solution (2.6 M) in order to observe the appearance of the microspheres (Figure 3). This can be explained by the acidity of the xylose extract solution, which comes from the treatment of the almond shells used to obtain it and favours the formation of microspheres.

Electron density maps of the elements were acquired by EDX coupled with the ESEM equipment for all samples. Table 1 summarizes the wt % of the elements obtained from the EDX microanalysis. Figures 8 and 9 depict the ESEM image and C, O, and S mapping obtained by EDX for the samples X60-S(2.6) and X15-biomass, respectively.

Table 1. Quantification of the elements of the carbon microspheres by ESEM-EDX.

Sample	C (wt %)	O (wt %)	S (wt %)	P (wt %)
S15	69.3	30.7	--	--
S60	71.1	28.9	--	--
G60-S	66.5	33.5	--	--
G60-P25	68.3	31.5	--	0.2
G60-(2.6)	71.6	28.4	--	--
G60-S(2.6)	73.7	26.2	--	--
G60-P(2.6)	67.4	32.6	--	--
G60-P25(2.6)	72.3	27.6	--	0.1
X60-S	64.6	35.4	--	--
X60-P	69.3	30.7	--	--
X60-P25	66.5	33.4	--	0.1
X60-(2.6)	72.0	28.0	--	--
X60-S(2.6)	71.2	28.7	0.10	--
X60-P(2.6)	72.2	27.8	--	--
X60-P25(2.6)	67.9	31.9	--	0.2
X120-S(2.6)	72.6	27.1	0.30	--
X120-P25(2.6)	74.6	25.3	--	0.2
X15-biomass	67.5	32.9	0.04	--
X60-biomass	67.5	32.5	0.05	--

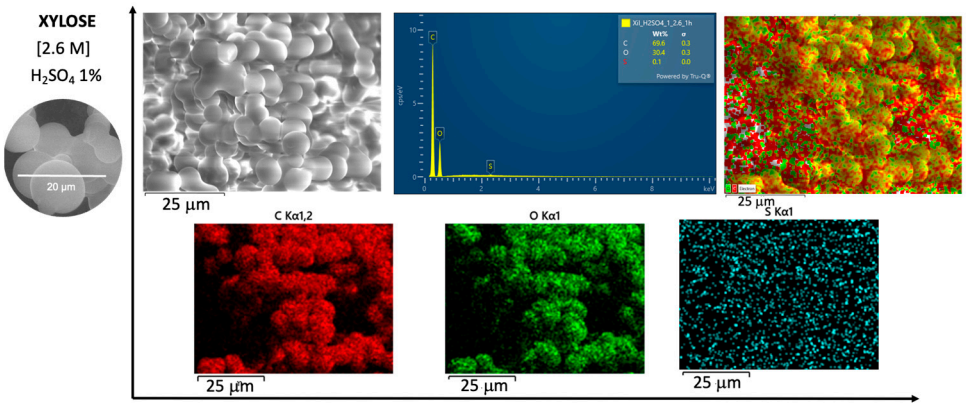

Figure 8. ESEM image and C, O, and S mapping obtained by EDX for the sample X60-S(2.6).

All samples showed values of 66–76% for C and of 25–35% for O (Table 1). This means that the microspheres were not only formed by carbon but also contained volatile organic compounds, as expected due to the low temperature used for the carbonization treatment: 180 °C. Only at higher carbonization temperatures (above 600–700 °C), can volatiles be avoided. In addition to C and O, all the microspheres prepared with the addition of 25% H_3PO_4 had P in small amounts (0.1–0.2%), and the microspheres prepared with

commercial xylose with 1% H_2SO_4 at a higher concentration (2.6 M) showed the presence of S in small amounts (0.1–0.3%) (Table 1, Figure 7). The microspheres prepared with aqueous solutions of xylose extracted from almond shells also contained S in very small amounts (0.04–0.05%) (Table 1, Figure 8), as a result of the acid medium (1% *v*/*v* H_2SO_4) used during the extraction of xylose from the lignocellulosic biomass.

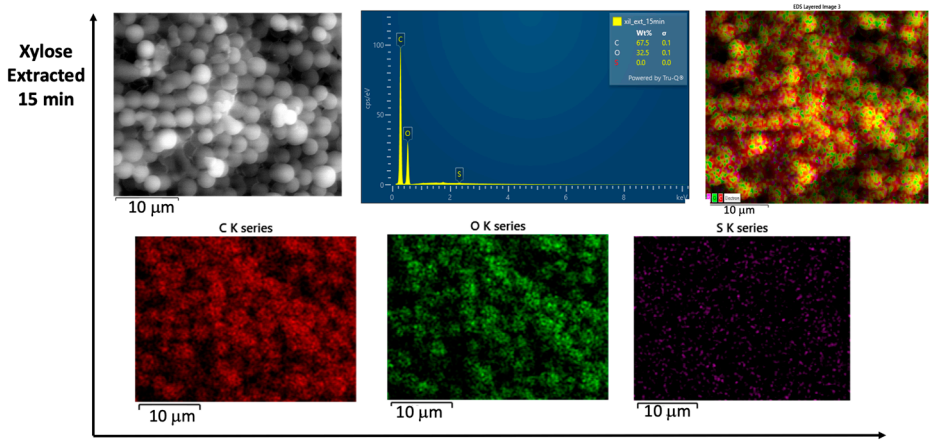

Figure 9. ESEM image and C, O, and S mapping obtained by EDX for the sample X15-biomass.

Proximate analysis was performed by TGA to quantify the content of fixed carbon in the precursor and in the spherical carbons prepared with microwave irradiation, first under a N_2 atmosphere to measure their moisture and volatile compounds content and then under an air atmosphere to determine their fixed carbon and ash content. Figure 10 shows the proximate analysis for commercial xylose and for the X120-P25(2.6) sample, as representative carbon microspheres obtained under microwaves.

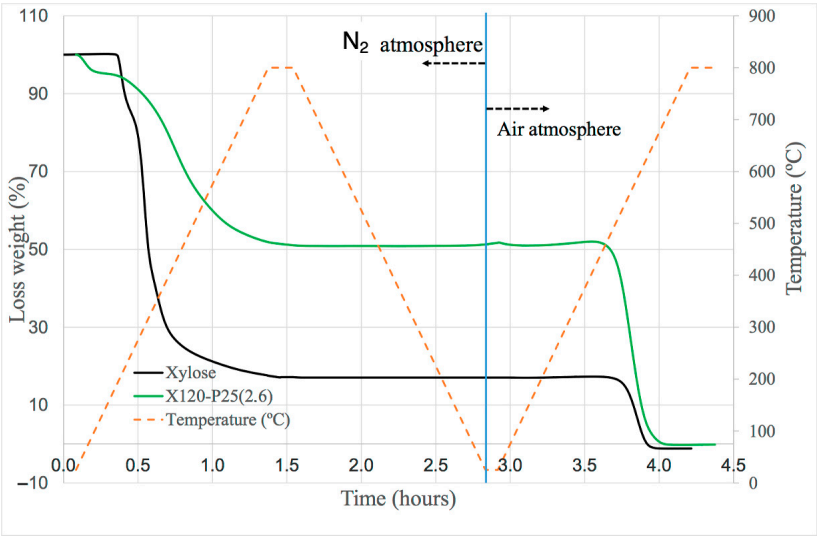

Figure 10. TGA study of commercial xylose and X120-P25(2.6) sample.

From the results, we can observe that commercial xylose had around 10% moisture and 74% volatile compounds, whereas the fixed carbon was around 16–18%, and as expected, the ash content was not observed. In contrast, the X120-P25(2.6) sample had around 7% moisture, 43% volatile compounds, and close to 50% fixed carbon. Such an increase in fixed carbon is expected due to its incorporation into the microspheres, and could give the material potential as a precursor in the obtention of activated carbons. The importance of using microwaves for obtaining carbon spheres with a high fixed carbon content should be

highlighted from economic and environmental perspectives, since the time and temperature of the hydrothermal process were considerably reduced in comparison with those prepared in conventional processes, in which the temperature for obtaining carbonized materials were above 600–700 °C.

FTIR spectra of the samples (e.g., Figure 11) showed typical organic groups related to the starting materials used to prepare microspheres, as previously observed by other authors [61,62]. The bands in the range 3034–2773 cm^{-1}, 1832–1580 cm^{-1}, and 1539–1345 cm^{-1} could be assigned to CH_2 units, C=O bond stretching vibrations, and C=C bond stretching in aromatic rings, respectively [61]. Moreover, one band at 1150 cm^{-1} could be attributed to C-O bond stretching vibration, and a small band at 740 cm^{-1} to C-H bond bending vibrations in aromatic rings. Samples prepared in sulfuric acid medium, as the samples of Figure 11, also showed one band at 1020 cm^{-1} assigned to S=O bond vibrations. Interestingly, X15-biomass showed a broad band at 3400 cm^{-1} assigned to O-H bond stretching vibrations and an additional C-O stretching band at 1100 cm^{-1}, which was not observed in X60-S(2.6), indicating a higher number of surface functional groups featuring C-O bonds. This could be explained by the higher oxygen content of the former, which was possibly caused by its smaller microsphere size reducing the proportion of carbon, found in the core of the spheres, to the oxygen found on their surface [62].

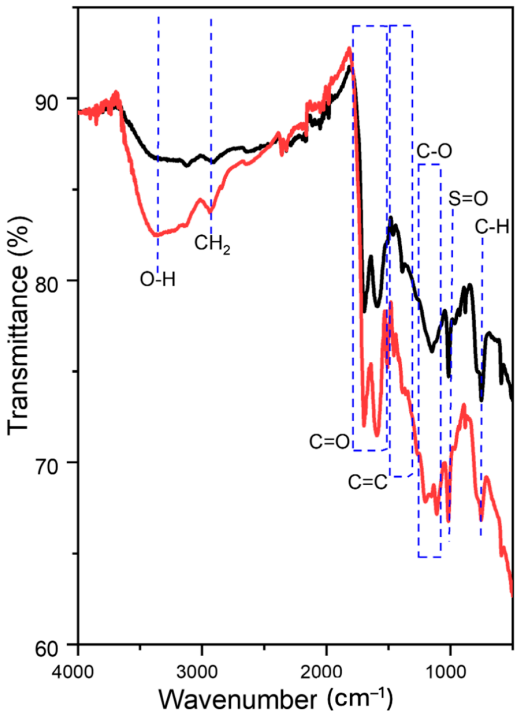

Figure 11. FTIR spectra of samples X60-S(2.6) (black) and X15-biomass (red).

Raman spectroscopy is usually employed to study the graphitic nature of carbon materials. The Raman scattering spectra of three representative microsphere samples are shown in Figure 12. Samples X60-S(2.6) and X60-Biomass produced spectra featuring a clear G-band at around 1580 cm^{-1}, caused by the vibration of sp^2 carbon atoms in a graphite-like lattice, and a D-band at around 1320 cm^{-1} associated with the vibration of out-of-plane carbon atoms in defects in the graphite lattice, indicating a relatively well-defined structure containing both graphitic and disordered carbon [61,62] in line with the typical structure observed in this type of material [61,62]. Both samples showed a D-band to G-band intensity ratio above 1, signalling a greater proportion of disordered carbon; however, this ratio was considerably larger for X60-Biomass, possibly due to the lower

xylose concentration during its preparation hampering the formation of graphitic domains. X15-Biomass produced a spectrum devoid of any significant features, indicating a much less defined carbon structure, likely as a consequence of its lower synthesis time.

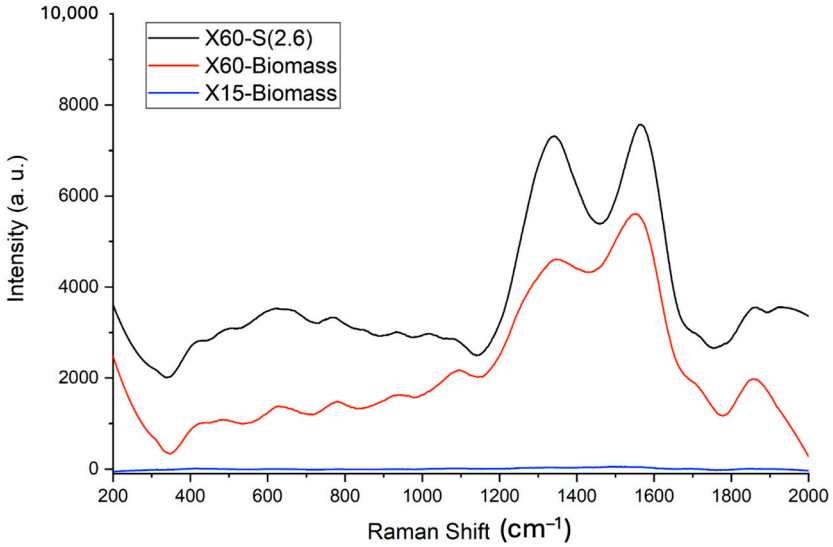

Figure 12. Smoothed Raman scattering spectra of X60-S(2.6), X15-Biomass, and X60-Biomass samples.

Using CO_2 to activate carbon materials is a sustainable, environmentally friendly alternative to conventional methods. Unlike chemical activation, physical activation with CO_2 avoids the use of hazardous reagents and enables efficient processing at moderate temperatures. This method is consistent with the principles of the circular economy, as it converts low-value organic waste and converts captured CO_2 into high-value activated carbons for use in environmental and industrial applications.

The textural properties of the microspherical carbon X60-biomass were developed through physical activation with CO_2 at 680 °C for 5 h (X60-biomass-AC5), 10 h (X60-biomass-AC10) and 20 h (X60-biomass-AC20). Figure 13 shows the N_2 adsorption–desorption isotherms and pore size distribution graphics, while Table 2 depicts the BET surface area, average pore diameter and pore volume values of the activated carbons with respect to the non-activated carbon precursor.

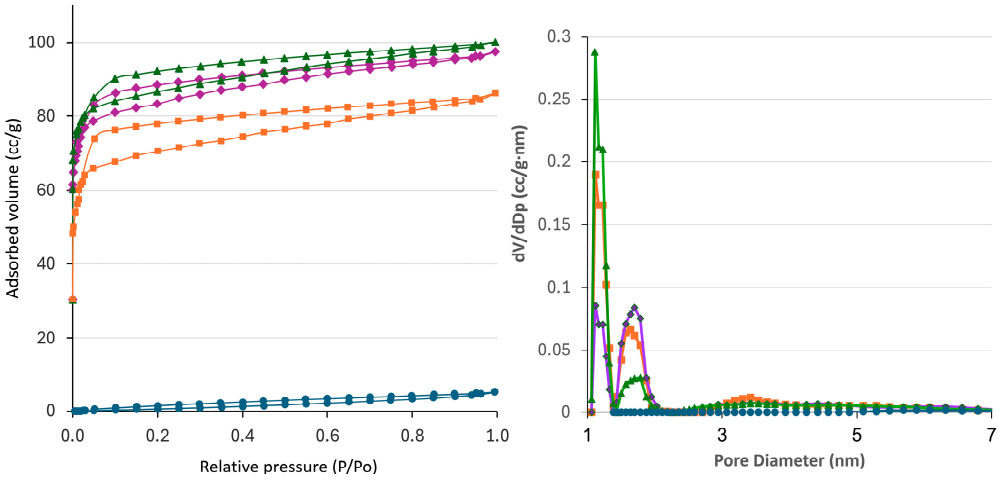

Figure 13. N_2 adsorption–desorption isotherms (left) and pore size distribution graphic (right) of the activated carbon samples X60-biomass-AC5 (orange), X60-biomass-AC10 (magenta), and X60-biomass-AC20 (green) with respect to the non-activated sample X-60-biomass (blue).

Table 2. Surface properties of the activated and non-activated carbon samples.

Sample	B.E.T. Surface Area (m^2/g)	Average Pore Size (nm)	Micropore Volume (cc/g)
X60-biomass	5	6.0	0.007
X60-biomass-AC5	243	1.1	0.129
X60-biomass-AC10	258	1.1	0.144
X60-biomass-AC20	326	1.1	0.148

The N_2 adsorption–desorption isotherms of the activated samples were of type I, which corresponded to microporous materials, according to the Brunauer, Emmett, and Teller classification, while the non-activated carbon microspheres did not show practical N_2 adsorption, likely due to their very low porosity (Figure 13, left). This is reinforced by the pore size distribution shown by the activated samples, which feature a large number of micropores with an extremely narrow size distribution centred around 1.1 nm alongside a smaller number of pores with sizes between 1.5 nm and 2 nm regardless of the activation conditions used (Figure 13, right) while non-activated carbon microspheres showed a very small number of pores.

After activation with CO_2, the surface area considerably increased regardless of the used conditions, growing over fifty–sixty times from the non-activated carbon microspheres to the activated ones, which gave these carbonaceous materials great potential to be used as catalytic supports. However, the increase in the treatment time did not have a great effect on the surface area, which only slightly increased at a longer time (Table 2). Additionally, a higher micropore volume and lower average pore size values were observed for the activated samples. This confirms the generation of narrower micropores during the activation of the samples, as previously observed for carbon microspheres prepared by conventional heating [3]. Activated carbon microspheres also showed much higher pore volumes than non-activated ones (Table 2), demonstrating the effectiveness of CO_2 activation in the formation of porosity in carbonaceous materials.

Figure 14 shows the Raman spectra of the activated sample X60-Biomass-AC5 compared to the same sample without activation (X60-biomass). Highly defined D and G bands were observed for the activated sample, implying a much more defined structure, although with a similar proportion of disordered and graphitic carbon. The increased structural definition of the activated microspheres can be explained by the high temperature of the activation process and is consistent with previous characterisations of microspheres subjected to high-temperature activation [61].

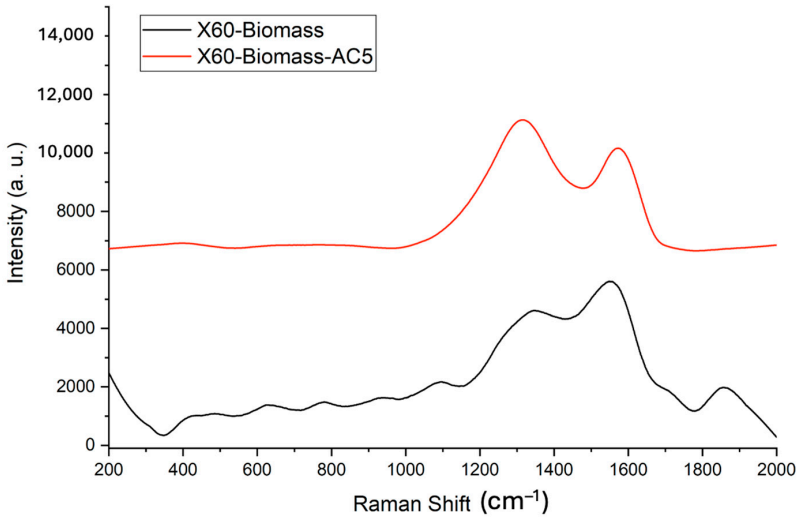

Figure 14. Smoothed Raman scattering spectra of X60-Biomass and X60-Biomass-AC5.

3. Materials and Methods

3.1. Materials

Three commercial carbohydrates, two monosaccharides (Xylose and D-(+)-Glucose) and one disaccharide (D-(+)-Saccharose) were used as precursors for the preparation of spherical carbons. Xylose (99%), D-(+)-Glucose (99%), and D-(+)-Saccharose (98%) were supplied by Merck KGaA (Darmstadt, Germany). Almond shells supplied by Cooperativa Unió nuts (Reus, Spain) were used as precursor to obtain xylose solutions.

3.2. Methods

3.2.1. Preparation of Xylose Extract Solution from Almond Shells

Xylose extract solutions were obtained from almond shells following a procedure described elsewhere [63]. Next, 5–15 g of ground almond shells were mixed in 50 mL of 1% (*m*/*v*) H_2SO_4 solution in a sealed Teflon reactor and heated to 120 °C for 1 h with microwave irradiation under magnetic stirring in a Milestone ETHOS-Touch Control laboratory microwave oven equipped with a temperature controller and operating at a frequency of 2.45 GHz. The solid obtained was filtered and the liquid phase was stored as "extract" in the fridge. The concentration of xylose in the extract solution was 36 g/L, as determined by HPLC chromatography with a RI detector using a RezexRHM-Monosaccharide H+(8%) column.

3.2.2. Preparation of Microspherical Carbons

Table 3 summarizes the preparation conditions and nomenclature of the synthesized samples. Firstly, 25 mL of a 1.6 M aqueous solution of commercial carbohydrate (glucose, xylose or saccharose) was added to a 100 mL sealed Teflon reactor and subjected to hydrothermal treatment at 180 °C for 15 min or 60 min under magnetic stirring in the previously described microwave oven, with a programmed power of 800 W and a heating rate of roughly 10 °C/min.

Table 3. Preparation conditions of the samples.

Sample Name	Carbohydrate	Carbohydrate Concentration	Reaction Medium	Heating	Heating Time (min)
S15	Saccharose	1.6 M	H_2O	Mw	15
S60	Saccharose	1.6 M	H_2O	Mw	60
G15	Glucose	1.6 M	H_2O	Mw	15
G60	Glucose	1.6 M	H_2O	Mw	60
X15	Xylose	1.6 M	H_2O	Mw	15
X60	Xylose	1.6 M	H_2O	Mw	60
G60-S	Glucose	1.6 M	1% *v*/*v* H_2SO_4	Mw	60
G60-P	Glucose	1.6 M	1% *v*/*v* H_3PO_4	Mw	60
G60-P25	Glucose	1.6 M	25% *v*/*v* H_3PO_4	Mw	60
G60(2.6)	Glucose	2.6 M	H_2O	Mw	60
G60-S(2.6)	Glucose	2.6 M	1% *v*/*v* H_2SO_4	Mw	60
G60-P(2.6)	Glucose	2.6 M	1% *v*/*v* H_3PO_4	Mw	60
G60-P25(2.6)	Glucose	2.6 M	25% *v*/*v* H_3PO_4	Mw	60
X60-S	Xylose	1.6 M	1% *v*/*v* H_2SO_4	Mw	60
X60-P	Xylose	1.6 M	1% *v*/*v* H_3PO_4	Mw	60
X60-P25	Xylose	1.6 M	25% *v*/*v* H_3PO_4	Mw	60
X60(2.6)	Xylose	2.6 M	H_2O	Mw	60
X60-S(2.6)	Xylose	2.6 M	1% *v*/*v* H_2SO_4	Mw	60
X60-P(2.6)	Xylose	2.6 M	1% *v*/*v* H_3PO_4	Mw	60
X60-P25(2.6)	Xylose	2.6 M	25% *v*/*v* H_3PO_4	Mw	60
X120-S(2.6)	Xylose	2.6 M	1% *v*/*v* H_2SO_4	Mw	120

Table 3. *Cont.*

Sample Name	Carbohydrate	Carbohydrate Concentration	Reaction Medium	Heating	Heating Time (min)
X120-P25(2.6)	Xylose	2.6 M	25% v/v H_3PO_4	Mw	120
X60(2.6)C	Xylose	2.6 M	H_2O	Conv	60
X60-S(2.6)C	Xylose	2.6 M	1% v/v H_2SO_4	Conv	60
X60-P(2.6)C	Xylose	2.6 M	1% v/v H_3PO_4	Conv	60
X15-biomass	Xylose from almond shells	0.2 M	Extract acid aqueous medium	Mw	15
X60-biomass	Xylose from almond shells	0.2 M	Extract acid aqueous medium	Mw	60

Mw: microwaves; Conv: conventional heating.

Another series of samples were prepared with commercial glucose and xylose modifying the reaction medium by adding different mineral acids (1% v/v H_2SO_4, 1% v/v H_3PO_4, 25% v/v H_3PO_4) and varying the concentration of carbohydrate in the solution, which was either 1.6 M or 2.6 M. These two concentrations were selected based on their successful application in previous studies for the synthesis of carbon microspheres [3]. The hydrothermal treatment of these samples was carried out with microwave irradiation at 180 °C for 60 min under magnetic stirring. Two more samples were synthesized by microwave-assisted hydrothermal treatment of 2.6 M aqueous solutions of xylose with 1% H_2SO_4 or 25% H_3PO_4 at 180 °C for 120 min. Finally, three samples were prepared by conventional hydrothermal treatment of 2.6 M aqueous solutions of xylose without acid addition and with 1% H_2SO_4 or 1% H_3PO_4 in an autoclave at 180 °C for 60 min for comparison.

For the preparation of spherical carbons from natural xylose obtained from almond shells, 25 mL of the xylose extract solution (0.2 M), obtained as explained in Section 3.2.1, was added to a 100 mL capacity sealed Teflon reactor and heated under stirring with microwave irradiation to 180 °C for 15 or 60 min.

For all the preparations, after hydrothermal treatment, the solid was recovered by filtration, washed with distilled water, and dried in an oven at 110 °C for 12 h.

3.2.3. Activation of Microspherical Carbons

A flow of 80 mL/min of CO_2 was passed through the sample X60-biomass and heated at 10 °C/min from room temperature to 680 °C using different activation times: 5 h (X60-biomass-AC5), 10 h (X60-biomass-AC10) and 20 h (X60-biomass-AC20).

3.2.4. Characterization Techniques

Environmental scanning electron microscopy (ESEM) was employed to observe the morphology and the particle size of the prepared materials using a JEOL 6400 electron microscope (Peabody, MA, USA) (3.5 nm resolution at 20 kV) fitted with an energy-dispersive X-ray spectrometer (Inca-Energy, Oxford Instruments in Abingdon, Oxfordshire, United Kingdom), which allowed us to obtain electronic density maps of the elements present in the samples, and with a Si(Li) detector with 1.38 eV energy resolution.

N_2 adsorption–desorption isotherms of spherical carbon samples were obtained at −196 °C using a 3Flex Micromeritics Adsorption analyser (Norcross, GA, USA) with a value of 0.164 nm^2 for the cross-section of the N_2 molecule. Brunauer, Emmet, and Teller (B.E.T.) theory was applied to calculate the total surface area. Samples were degassed at 120 °C prior to analysis.

Proximate analysis was performed by thermogravimetric analyses (TGA). The experiments were carried out with a Mettler Toledo TGA 2 equipment (Columbus, AL, USA) to quantify the carbon content in the prepared materials. First, 20 mg of the sample was

heated at 10 °C/min under a N_2 flow (50 mL/min) from room temperature up to 800 °C, as described elsewhere [64]. This allows the determination of the sample moisture and volatile compounds content. The sample was then cooled to room temperature and submitted to a new temperature cycle in the same heating conditions but under airflow (50 mL/min) to determine the ash and fixed carbon content.

FT-IR spectra of samples were recorded with a JASCO FT-IR 6700 spectrometer (Barcelona, Spain) by attenuated total reflection with a diamond crystal. Each spectrum was built from 32 sample scans from 400 cm^{-1} to 4000 cm^{-1} with a 4 cm^{-1} resolution.

Raman scattering spectra of samples were recorded with a Renishaw InVia Raman confocal microscope (Barcelona, Spain) working with a near-infrared 785 nm laser source and measured from 200 cm^{-1} to 2000 cm^{-1} with a 1 cm^{-1} resolution.

4. Conclusions

The main advantages of using microwave irradiation for the preparation of carbon microspheres were as follows: (i) The carbonized materials were prepared much faster (15–60 min) and at lower temperature (180 °C) than by conventional heating (12–24 h and 600–700 °C, respectively, as reported in the literature). (ii) The heating and cooling rates were higher than those associated with the conventional method. Therefore, the amount of gases needed to maintain an inert atmosphere could be reduced. (iii) Adding acid medium under microwaves increased the formation rate of the carbons. (iv) The activation of the carbon microspheres with CO_2 resulted in high-surface-area materials (243–326 m^2/g) with great potential as catalytic supports.

Author Contributions: Conceptualization, A.J.R.-A. and Y.C.; methodology, A.J.R.-A. and M.D.G.; validation, J.G.-R. and Y.C.; investigation, A.J.R.-A., J.G.-R. and L.E.A.-H.; writing—original draft preparation, A.J.R.-A., M.D.G. and Y.C.; writing—review and editing, Y.C.; visualization, M.D.G. and Y.C.; supervision, J.G.-R. and Y.C.; funding acquisition, A.J.R.-A. and Y.C. All authors have read and agreed to the published version of the manuscript.

Funding: This research was funded by the project PID2019-110735RB-C22 funded by MCIU/AEI/10.13039/501100011033. Dr. A. J. Romero-Anaya thanks European Union's Horizon 2020 research and innovation programme under Marie Sklodowska Curie grant agreement No712949, Generalitat de Catalunya, TECNIOspring project TECSPR18-1-0051, for the financial support provided during years 2019–2021. L. Arrieche-Hernández also thanks Generalitat de Catalunya for the grant 2024 FI-1 00418.

Data Availability Statement: The original contributions presented in the study are included in the article. Further inquiries can be directed to the corresponding author/s.

Conflicts of Interest: The authors declare no conflicts of interest. The funders had no role in the design of the study; in the collection, analyses, or interpretation of data; in the writing of the manuscript; or in the decision to publish the results.

Abbreviations

The following abbreviations are used in this manuscript:

CONV	Conventional heating
EDX	Energy Dispersive X-ray spectroscopy
ESEM	Environmental scanning electron microscopy
GLU	Glucose
5-HMF	5-Hydroxymethylfurfural
MW	Microwaves
SAC	Saccharose
TGA	Thermogravimetry
XYL	Xylose

References

1. Yenisoy-Karakaş, S.; Aygün, A.; Güneş, M.; Tahtasakal, E. Physical and chemical characteristics of polymer-based spherical activated carbon and its ability to adsorb organics. *Carbon* **2004**, *42*, 477–484. [CrossRef]
2. Romero-Anaya, A.J.; Lillo-Ródenas, M.A.; Linares-Solano, A. Spherical activated carbons for low concentration toluene adsorption. *Carbon* **2010**, *48*, 2625–2633. [CrossRef]
3. Romero-Anaya, A.J.; Ouzzine, M.; Lillo-Ródenas, M.A.; Linares-Solano, A. Spherical carbons: Synthesis, characterization and activation processes. *Carbon* **2014**, *68*, 296–307. [CrossRef]
4. Liu, J.; Wickramaratne, N.P.; Qiao, S.Z.; Jaroniec, M. Molecular-based design and emerging applications of nanoporous carbon spheres. *Nat. Mater.* **2015**, *14*, 763–774. [CrossRef]
5. Bedin, K.C.; Cazetta, A.L.; Souza, I.P.A.F.; Pezoti, O.; Souza, L.S.; Souza, P.S.C.; Yokoyama, J.T.C.; Almedia, V.C. Porosity enhancement of spherical activated carbon: Influence and optimization of hydrothermal synthesis conditions using response surface methodology. *J. Environ. Chem. Eng.* **2018**, *6*, 991–999. [CrossRef]
6. Ouzzine, M.; Romero-Anaya, A.J.; Lillo-Ródenas, M.A.; Linares-Solano, A. Spherical activated carbons for the adsorption of a real multicomponent VOC mixture. *Carbon* **2019**, *148*, 214–223. [CrossRef]
7. Bedin, K.C.; Souza, I.P.A.F.; Cazetta, A.L.; Spessato, L.; Ronix, A.; Almeida, V.C. CO_2-spherical activated carbon as a new adsorbent for Methylene Blue removal: Kinetic, equilibrium and thermodynamic studies. *J. Mol. Liq.* **2018**, *269*, 132–139. [CrossRef]
8. Zhang, Q.; Meng, Y.; Bai, Y.; Li, M. Sulfur and nitrogen in-situ co-doped hierarchical spherical porous carbon for efficient lithium storage. *J. Electroanal. Chem.* **2020**, *862*, 114013. [CrossRef]
9. Sun, N.; Sun, C.; Liu, H.; Liu, J.; Stevens, L.; Drage, T.; Snape, C.E.; Li, K.; Wei, W.; Sun, Y. Synthesis, characterization and evaluation of activated spherical carbon materials for CO_2 capture. *Fuel* **2013**, *113*, 854–862. [CrossRef]
10. Eguchi, M.; Okubo, A.; Yamamoto, S.; Kikuchi, M.; Uno, K.; Kobayashi, Y.; Nishitani-Gamo, M.; Ando, T. Preparation of catalyst for a polymer electrolyte fuel cell using a novel spherical carbon support. *J. Power Sources* **2010**, *195*, 5862–5867. [CrossRef]
11. Ouzzine, M.; Romero-Anaya, A.J.; Lillo-Ródenas, M.A.; Linares-Solano, A. Spherical activated carbon as an enhanced support for TiO_2/AC photocatalysts. *Carbon* **2014**, *67*, 104–118. [CrossRef]
12. Zhang, Y.; Yang, L.; Yan, L.; Wang, G.; Liu, A. Recent advances in the synthesis of spherical and nanoMOF-derived multifunctional porous carbon for nanomedicine applications. *Coord. Chem. Rev.* **2019**, *391*, 69–89. [CrossRef]
13. Saleh, T.A.; Ali, I. Synthesis of polyamide grafted carbon microspheres for removal of rhodamine B dye and heavy metals. *J. Environ. Chem. Eng.* **2018**, *6*, 5361–5368. [CrossRef]
14. Fang, Y.; Liu, L.; Xiang, H.; Wang, Y.; Sun, X. Biomass-based carbon microspheres for removing heavy metals from the environment: A review. *Mater. Today Sustain.* **2022**, *18*, 100136. [CrossRef]
15. Zhu, J.; Liao, L.; Bian, X.; Kong, J.; Yang, P.; Liu, B. pH-Controlled Delivery of Doxorubicin to Cancer Cells, Based on Small Mesoporous Carbon Nanospheres. *Small* **2012**, *8*, 2715–2720. [CrossRef] [PubMed]
16. Tagliavini, M.; Schäfer, A.I. Removal of steroid micropollutants by polymer-based spherical activated carbon (PBSAC) assisted membrane filtration. *J. Hazard. Mater.* **2018**, *353*, 514–521. [CrossRef] [PubMed]
17. Wang, X.; Zhou, J.; Xing, W.; Liu, B.; Zhang, J.; Lin, H.; Cui, H.; Zhuo, S. Resorcinol–formaldehyde resin-based porous carbon spheres with high CO_2 capture capacities. *J. Energy Chem.* **2017**, *26*, 1007–1013. [CrossRef]
18. Wang, Q.; Liang, X.Y.; Zhang, R.; Liu, C.J.; Liu, X.J.; Qiao, W.; Zhan, L.; Ling, L. Preparation of polystyrene-based activated carbon spheres and their adsorption of dibenzothiophene. *New Carbon Mater.* **2009**, *24*, 55–60. [CrossRef]
19. Wang, D.; Chen, M.; Wang, C.; Bai, J.; Zheng, J. Synthesis of carbon microspheres from urea formaldehyde resin. *Mater. Lett.* **2011**, *65*, 1069–1072. [CrossRef]
20. Romero-Anaya, A.J.; Lillo-Ródenas, M.A.; Salinas-Martínez de Lecea, C.; Linares-Solano, A. Hydrothermal and conventional H_3PO_4 activation of two natural bio-fibers. *Carbon* **2012**, *50*, 3158–3169. [CrossRef]
21. Chen, W.H.; Ye, S.C.; Sheen, H.K. Hydrothermal carbonization of sugarcane bagasse via wet torrefaction in association with microwave heating. *Bioresour. Technol.* **2012**, *118*, 195–203. [CrossRef] [PubMed]
22. Luo, G.; Shi, W.; Chen, X.; Ni, W.; Strong, P.J.; Jia, Y.; Wang, H. Hydrothermal conversion of water lettuce biomass at 473 or 523 K. *Biomass Bioenergy* **2011**, *35*, 4855–4861. [CrossRef]
23. Jiahao, W.; Weiquan, C. One-step hydrothermal preparation of N-doped carbon spheres from peanut hull for efficient removal of Cr(VI). *J. Environ. Chem. Eng.* **2020**, *8*, 104449. [CrossRef]
24. Heilmann, S.M.; Davis, H.T.; Jader, L.R.; Lefebvre, P.A.; Sadowsky, M.J.; Schendel, F.J.; von Keitz, M.G.; Valentasa, K.J. Hydrothermal carbonization of microalgae. *Biomass Bioenergy* **2010**, *34*, 875–882. [CrossRef]
25. AnhCao, K.L.; Rahmatika, A.M.; Kitamoto, Y.; Nguyen, M.T.T.; Ogi, T. Controllable synthesis of spherical carbon particles transition from dense to hollow structure derived from Kraft lignin. *J. Colloid Interface Sci.* **2021**, *589*, 252–263. [CrossRef]
26. Sevilla, M.; Fuertes, A.B. The production of carbon materials by hydrothermal carbonization of cellulose. *Carbon* **2009**, *47*, 2281–2289. [CrossRef]

27. Wang, F.L.; Pang, L.L.; Jiang, Y.Y.; Chen, B.; Lin, D.; Lun, N.; Zhu, H.L.; Liu, R.; Meng, X.L.; Wang, Y.; et al. Simple synthesis of hollow carbon spheres from glucose. *Mater. Lett.* **2009**, *63*, 2564–2566. [CrossRef]
28. Gámez, S.; Lozada, A.B.; Guevara, A.; de la Torre, E. A green and easy way for carbon microspheres synthesis impregnated with palladium for hexavalent chromium reduction. *J. Environ. Chem. Eng.* **2019**, *7*, 103467. [CrossRef]
29. Yao, C.; Shin, Y.; Wang, L.Q.; Windisch, C.F.; Samuels, W.D.; Arey, B.W.; Wang, C.; Risen, W.M.; Exarhox, G.J. Hydrothermal Dehydration of Aqueous Fructose Solutions in a Closed System. *J. Phys. Chem. C* **2007**, *111*, 15141–15145. [CrossRef]
30. Titirici, M.M.; Antonietti, M.; Baccile, N. Hydrothermal carbon from biomass: A comparison of the local structure from poly- to monosaccharides and pentoses/hexoses. *Green Chem.* **2008**, *10*, 1204–1212. [CrossRef]
31. Funke, A.; Ziegler, F. Hydrothermal carbonization of biomass: A summary and discussion of chemical mechanisms for process engineering. *Biofuel Bioprod Biorefin.* **2010**, *4*, 160–177. [CrossRef]
32. Román, S.; Nabais, J.M.V.; Laginhas, C.; Ledesma, B.; González, J.F. Hydrothermal carbonization as an effective way of densifying the energy content of biomass. *Fuel Process. Technol.* **2012**, *103*, 78–83. [CrossRef]
33. Guiotoku, M.; Rambo, C.R.; Hansel, F.A.; Magalhães, W.L.E.; Hotza, D. Microwave-assisted hydrothermal carbonization of lignocellulosic materials. *Mater. Lett.* **2009**, *63*, 2707–2709. [CrossRef]
34. Toor, S.S.; Rosendahl, L.; Rudolf, A. Hydrothermal liquefaction of biomass: A review of subcritical water technologies. *Energy* **2011**, *36*, 2328–2342. [CrossRef]
35. Schuhmacher, J.P.; Huntjens, F.J.; Van-Krevelen, D.W. Chemical structure and properties of coal XXVI—Studies on artificial coalification. *Fuel* **1960**, *39*, 223–234.
36. Berl, E.; Schimdt, A. Die Inkohlung von cellulose und lignin in neutralem medium. *Liebigs Ann. Chem.* **1932**, *493*, 97–123. [CrossRef]
37. Wang, Q.; Li, H.; Chen, L.; Huang, X. Monodispersed hard carbon spherules with uniform nanopores. *Carbon* **2001**, *39*, 2211–2214. [CrossRef]
38. Sun, X.; Li, Y. Ga_2O_3 and GaN semiconductor hollow spheres. *Angew. Chem. Int. Ed. Engl.* **2004**, *43*, 3827–3831. [CrossRef]
39. Sevilla, M.; Maciá-Agulló, J.A.; Fuertes, A.B. Hydrothermal carbonization of biomass as a route for the sequestration of CO_2: Chemical and structural properties of the carbonized products. *Biomass Bioenergy* **2011**, *35*, 3152–3159. [CrossRef]
40. Sevilla, M.; Fuertes, A.B. Chemical and Structural Properties of Carbonaceous Products Obtained by Hydrothermal Carbonization of Saccharides. *Chem. Eur. J.* **2009**, *15*, 4195–4203. [CrossRef]
41. Sevilla, M.; Lota, G.; Fuertes, A.B. Saccharide-based graphitic carbon nanocoils as supports for PtRu nanoparticles for methanol electrooxidation. *J. Power Sources* **2007**, *171*, 546–551. [CrossRef]
42. Zhao, L.; Baccile, N.; Gross, S.; Zhang, Y.; Wei, W.; Sun, Y.; Antonietti, M.; Titirici, M.M. Sustainable nitrogen-doped carbonaceous materials from biomass derivatives. *Carbon* **2010**, *48*, 3778–3787. [CrossRef]
43. Falco, C.; Baccile, N.; Titirici, M.M. Morphological and structural differences between glucose, cellulose and lignocellulosic biomass derived hydrothermal carbons. *Green Chem.* **2011**, *13*, 3273–3281. [CrossRef]
44. Baccile, N.; Laurent, G.; Babonneau, F.; Fayon, F.; Titirici, M.M.; Antonietti, M. Structural characterization of hydrothermal carbon spheres by advanced solid-state MAS 13C NMR investigations. *J. Phys. Chem. C* **2009**, *113*, 9644–9654. [CrossRef]
45. Demir-Cakana, R.; Makowski, P.; Antonietti, M.; Goettmann, F.; Titirici, M.M. Hydrothermal synthesis of imidazole functionalized carbon spheres and their application in catalysis. *Catal. Today* **2010**, *150*, 115–118. [CrossRef]
46. Yu, L.; Brun, N.; Sakaushi, K.; Eckert, J.; Titirici, M.M. Hydrothermal nanocasting: Synthesis of hierarchically porous carbon monoliths and their application in lithium–sulfur batteries. *Carbon* **2013**, *61*, 245–253. [CrossRef]
47. Matos, J.; Rosales, M.; Demir-Cakan, R.; Titirici, M.M. Methane conversion on Pt–Ru nanoparticles alloy supported on hydrothermal carbon. *Appl. Catal. A Gen.* **2010**, *386*, 140–146. [CrossRef]
48. Laszlo, T.S. Industrial applications of microwaves. *Phys. Teach.* **1980**, *18*, 570–579. [CrossRef]
49. Gebretsadik, F.B.; Mance, D.; Baldus, M.; Salagre, P.; Cesteros, Y. Microwave synthesis of delaminated acid saponites using quaternary ammonium salt or polymer as template. Study of pH influence. *Appl. Clay Sci.* **2015**, *114*, 20–30. [CrossRef]
50. Granados-Reyes, J.; Salagre, P.; Cesteros, Y. Effect of microwaves, ultrasounds and interlayer anion on the hydrocalumites synthesis. *Micropor. Mesopor. Mater.* **2014**, *199*, 117–124. [CrossRef]
51. Sánchez, T.; Salagre, P.; Cesteros, Y. Ultrasounds and microwave-assisted synthesis of mesoporous hectorites. *Micropor. Mesopor. Mater.* **2013**, *171*, 24–34. [CrossRef]
52. Salema, A.A.; Ani, F.N. Microwave induced pyrolysis of oil palm biomass. *Bioresour Technol.* **2011**, *102*, 3388–3395. [CrossRef]
53. Cheng, Y.; Li, B.; Huang, Y.; Wang, Y.; Chen, J.; Wei, D.; Feng, Y.; Jia, D.; Zhou, Y. Molten salt synthesis of nitrogen and oxygen enriched hierarchically porous carbons derived from biomass via rapid microwave carbonization for high voltage supercapacitors. *Appl. Surf. Sci.* **2018**, *439*, 712–723. [CrossRef]
54. Liew, R.K.; Chai, C.; Yek, P.N.Y.; Phang, X.Y.; Chong, M.Y.; Nam, W.L.; Su, M.H.; Lam, W.H.; Ma, N.L.; Lam, S.S. Innovative production of highly porous carbon for industrial effluent remediation via microwave vacuum pyrolysis plus sodium-potassium hydroxide mixture activation. *J. Clean. Prod.* **2019**, *208*, 1436–1445. [CrossRef]

55. Menéndez, J.A.; Arenillas, A.; Fidalgo, B.; Fernández, Y.; Zubizarreta, L.; Calvo, E.G.; Bermúdez, J.M. Microwave heating processes involving carbon materials. *Fuel Process Technol.* **2010**, *91*, 1–8. [CrossRef]
56. Shi, N.; Liu, Q.; He, X.; Wang, G.; Chen, N.; Peng, J.; Ma, L. Molecular structure and formation mechanism of hydrochar from hydrothermal carbonization of carbohydrates. *Energy Fuels* **2019**, *33*, 9904–9915. [CrossRef]
57. van Zandvoort, I.; Wang, Y.; Rasrendra, C.B.; van Eck, E.R.H.; Bruijnincx, P.C.A.; Heeres, H.J.; Weckhuysen, B.M. Formation, molecular structure, and morphology of humins in biomass conversion: Influence of feedstock and processing conditions. *ChemSusChem* **2013**, *6*, 1745–1758. [CrossRef]
58. Falco, C.; Perez Caballero, F.; Babonneau, F.; Gervais, C.; Laurent, G.; Titirici, M.M.; Baccile, N. Hydrothermal carbon from biomass: Structural differences between hydrothermal and pyrolyzed carbons via 13C solid state NMR. *Langmuir* **2011**, *27*, 14460–14471. [CrossRef]
59. Titirici, M.-M. *Sustainable Carbon Materials from Hydrothermal Processes*, 1st ed.; John Wiley & Sons, Ltd.: Hoboken, NJ, USA, 2013; pp. 75–100. [CrossRef]
60. Xiang, Q.; Lee, Y.; Torget, R. Kinetics of glucose decomposition during dilute-acid hydrolysis of lignocellulosic biomass. *Appl. Biochem. and Biotechnol.* **2004**, *115*, 1127–1138. [CrossRef]
61. Li, K.; Liu, S.; Shu, T.; Yan, L.; Guo, H.; Dai, Y.; Luo, X.; Luo, S. Fabrication of carbon microspheres with controllable porous structure by using waste Camellia oleifera shells. *Mater. Chem. Phys.* **2016**, *181*, 518–528. [CrossRef]
62. Wang, S.; Yue, X.; Zhao, X.; Yuan, H. Preparation of a carbon microsphere-based solid acid application to waste frying oil transesterification. *Diam. Relat. Mater.* **2021**, *116*, 108420. [CrossRef]
63. Sánchez, V.; Dafinov, A.; Salagre, P.; Llorca, J.; Cesteros, Y. Microwave-Assisted Furfural Production Using Hectorites and Fluorohectorites as Catalysts. *Catalysts* **2019**, *9*, 706. [CrossRef]
64. Muñoz-Guillena, M.J.; Linares-Solano, A.; Salinas-Martínez de Lecea, C. Determination of calorific values of coals by differential thermal analysis. *Fuel* **1992**, *71*, 579–583. [CrossRef]